# Influence of actual component characteristics on the optimal energy mix of a photovoltaic-wind-diesel hybrid system for a remote off-grid

Publisher's version at DOI: 10.1016/j.jclepro.2018.01.032

# Influence of actual component characteristics on the optimal energy mix of a PV-wind-diesel hybrid system for a remote off-grid application

Lorenzo Ferrari [1]*, Alessandro Bianchini [2a], Giacomo Galli [2b], Giovanni Ferrara [2c], Ennio Antonio Carnevale [2d]

[1] ***Department of Energy, Systems, Construction and Territory Engineering (DESTEC), University of Pisa***
Largo Lucio Lazzarino, 1, 56122, Pisa, Italy - Tel. +39 050 221 7132 - Fax +39 050 221 7333 - E-mail: lorenzo.ferrari@unipi.it

[2] ***Department of Industrial Engineering (DIEF), University of Florence***
Via di Santa Marta 3, 50139, Firenze, Italy - Tel. +39 055 275 8773 - Fax +39 055 275 8775 - E-mail: a) bianchini@vega.de.unifi.it, b) giacomo.galli@stud.unifi.it, c) giovanni.ferrara@unifi.it, d) ennio.carnevale@unifi.it

* = *contact author*

## Abstract

Hybrid energy systems are an interesting solution for the electrification of remote, off-grid users, which usually are obligated to satisfy their electricity demand by means of quite old technologies, like for example diesel generators. An energy mix including also renewable energy sources (such as wind and PV) would lead to a reduction of supply costs and is therefore being increasingly appreciated.

In the present study, a sizing strategy was developed based on a long-term energy production cost analysis, able to predict the optimum configuration of a hybrid PV-wind-diesel stand-alone system. With respect to conventional practical design approaches already available in the literature, a more realistic description of the problem was here provided, since the present analysis relies in the use of actual machines data, realistic system constraints and cost functions, which led to the identification of some trends that are usually neglected by the optimization processes using continuous variables for the power outputs of renewable energy sources.

The approach was tested on an isolated mountain chalet in Italian Alps. The hybrid system was optimized based on the maximum long-term saving with respect to a conventional diesel engine configuration. The results for this case study showed that the optimal solution was not that including the maximum allowed contribution from renewables, highlighting the existence of an optimized energy mix between the three sources. Accumulation batteries were also able to induce a reduction of both the fuel consumption and the engine transitory usage. According to the present results, a properly sized hybrid system could provide notable money and pollution savings for a remote consumer with respect to a diesel-only configuration.

**Keywords:** photovoltaic panel; wind turbine; battery; hybrid energy system; off-grid; optimization

## Nomenclature

| | | |
|---|---|---|
| $A$ | Total Area of Photovoltaic Panels | [m$^2$] |
| $A_{PV\_S}$ | Area of a Single Photovoltaic Panel | [m$^2$] |
| $b$ | Parameter for the Electronic Devices Cost | |
| $c_f$ | Initial Oil Price | [€] |
| $CN$ | Long Term Cost | [€] |
| $E$ | Energy | [kWh] |
| $e_f$ | Oil Price Annual Escalation Rate | |
| $FC_n$ | Fixed Maintenance and Operation Cost | [€] |

| | | |
|---|---|---|
| $G$ | Irradiance | [W/m$^2$] |
| $g_m$ | Annual Inflation Rate | |
| GPS | Global Positioning System | |
| $h$ | Hours of Functioning | [h] |
| $i$ | Return on Investment Index | |
| $IC$ | Installation Cost | [€] |
| $life$ | Lifetime | [h] |
| LTS | Long Term Savings | [€] |
| $m$ | Fixed O&M Costs Expressed as a Fraction of Initial Capital | |
| $M_f$ | Annual Fuel Consumption | [l] |
| $N_{PV}$ | Number of Photovoltaic Panels | |
| PA | Pinch Analysis | |
| PV | Photovoltaic Panels | |
| $P$ | Power | [W] |
| $P_{PVnom}$ | Power of Photovoltaic Panels | [W] |
| $P_{PV\_S}$ | Nominal Power of a Single Photovoltaic Panel | [W] |
| $P_{Wnom}$ | Power of the Wind Turbine | [W] |
| $Q$ | Capacity of the Battery Bank | [Ah] |
| $T_m$ | Temperature of the Photovoltaic Panel | [K] |
| $VC_n$ | Variable Maintenance and Operation Cost | [€] |

*Greek letters*

| | | |
|---|---|---|
| $\alpha$ | Specific Installation Cost of PV Panels | [€/kW] |
| $\gamma$ | Specific Installation Cost of the Diesel Generator | [€/kW] |
| $\Delta P$ | Power Lack/Surplus | [W] |
| $\eta_{nom}$ | Nominal Efficiency of Photovoltaic Panels | |
| $\eta_{rel}$ | Relative Efficiency of Photovoltaic Panels | |
| $\lambda$ | Parameter for the Electronic Devices Cost | |
| $\xi$ | Parameter for the Battery Bank Cost | |
| $\tau$ | Parameter for the Electronic Devices Cost | |
| $\omega$ | Parameter for the Battery Bank Cost | |

*Subscripts*

| | |
|---|---|
| *0* | Initial Investment |
| *BAT* | Battery |
| *DG* | Diesel Generator |
| *ELEC* | Electronic Components |
| *max* | Maximum |
| *min* | Minimum |
| *nom* | Nominal |
| *PV* | Photovoltaic Panel |
| *REN* | Renewables |
| *USER* | User |

## 1. Introduction

Renewable energy deployment in off-grid systems is continuously growing both in developed and developing countries. According to [1], 1.16 billion people globally still have no access to the electricity grid. About 95% of these people live in the sub-Saharan Africa and South and East Asia, with the remainder spread almost equally across Middle East, Central Asia and South America [2]. In spite of the average technological level, however, in 2009 there was still also a small part (about 0.5 million people) of the EU residents who had not direct access to a local utility network [3].

Even in case of developed countries there are areas where the it is not possible to be connected to the grid due to local electrical network scarcity in the area (e.g. remote areas) or due to the prohibitively high connection cost (e.g. 8000–11000 €/km [4]). Consequently, experiences of planned global rural electrification programs can be found in several countries [5-6], many of which include hybrid systems (e.g. [7]) integrating fossil fuels and renewable energies, managed following smart-grid approaches [8-9]. In particular, the larger and larger penetration of distributed renewable energy sources in micro-grids is leading the research to develop new and more refined strategies for a correct management of the power coming from renewables, especially focusing on forecasting models, demand response programs, accumulation systems and power routing models [10-13].

On the other hand, in many developing countries the population growth is far outpacing the extension of the grid. According to [14], the number of people living off the grid has grown by 114 million people on the African continent since 2000, with the absolute number that will continue to grow in the next decade. Off-grid renewable energy systems are then not only urgently needed to connect this vast number of people with a source of electricity, but also most appropriate to geographical constraints and cost for grid extension in many applications. At the same time, with declining cost and increasing performance for small hydro installations, solar photovoltaics (PV) and wind turbines, as well as declining costs and technological improvements in electricity storage and control systems, off-grid renewable energy systems could become an important growth market for the future deployment of renewables themselves. As discussed in [1], in the short- to medium-term, the market for off-grid renewable energy systems is expected to increase through the hybridization of existing diesel grids with wind, solar PV, biomass gasification and small hydropower, especially on islands and in rural areas. Furthermore, renewables in combination with batteries allow stand-alone operations and batteries are now a standard component of solar PV lighting systems and solar home systems (e.g. [15-16]). To this purpose, increasing interest is being paid by researchers and industrial manufacturers in further analyzing and optimizing these systems.

The motivation of the present study is to contribute to the development of robust techniques for a further development of design strategies for off-grid hybrid systems including renewables, batteries for energy storage and fossil-fuel generators. In particular, as will be shown later on, the purpose of the study is to show the impact on the best design trends of the real characteristics of the selected components.

By looking first at the relevant technical literature on the general topic of sizing and management of micro-grids and/or off-grid hybrid systems, it is apparent that it is extremely vast. Among others, a great impulse to the study of hybrid renewable energy systems was given by the team of Prof. J.K. Kaldellis of TEI of Piraeus (Greece), who established a robust approach for the energy mix selection in small grids like those of Greek islands [17-18], as a function of many parameters like, for example, long term wind data [4], wind potential classes [19] or minimum long-term electricity production cost [20].

Based on their experience, similar approaches have been replicated in the recent past by many researchers into different environments (e.g. [21-25]). The use of proper mixes of renewable energy sources also has some very interesting prospects in even smaller applications, i.e. in satisfying the energy demand of remote buildings [26] or residential complexes located in particular environments [27], far from the local electricity grid [28].

As correctly noticed by [16], from mathematical perspective, the sizing of a general hybrid energy system is “a constrained optimization problem that aims at minimizing an objective function subject to a set of constraints”. A first key element is then to identify the objective function to be optimized. With particular focus on single buildings or isolated users - like those investigated in the present study - one of the most common ones is of course the cost of energy consumption in the system [29]. The satisfaction of a given loading profile is the next class of objective functions [16]. In doing so, several additional functions can be related to the loading profile fulfillment, like peak shaving [30], load leveling and peak reducing [31], load shedding [32], and load shifting [33]. Minimizing environmental pollution can also be regarded as objective function [34].

A second important element to be considered is the sizing method, i.e. the modeling of the system under analysis, that is used to maximize one of the aforementioned functions. In this sense, recently some very interesting methods have been presented in the literature. For the sack of conciseness, the pinch analysis and the design space are here cited. Regarding the first, as discussed by [35], the pinch analysis (PA) “follows the laws of thermodynamics. The term ‘Pinch’ represents a bottleneck for feasible heat recovery and can be developed either by graphical or numerical methods”. When dealing with different systems, the PA can be referred to different quantities or sources in the system: an overview of methods and approaches of the powerful method of PA can be found in [36]. Another technique is represented by the definition of a design space, i.e. a collector of all the feasible solution for a given system based on different constraints, within which the selected solution can be looked for (e.g. [37] and [38]). This method will be used in the present study, where the long-term savings will be used as the objective function and the design space will be defined numerically based on the constraints shown later on.

Moving to the specific contribution of the present work, in the attempt of assessing a robust, but simple, approach to selection of the most promising energy mix for a remote off-grid users, a preliminary study of some of the present authors [39] has already assessed the feasibility of a hybrid energy system for the case study that will be used also for the present analysis. The hybrid system was composed by a diesel generator, PV panels, a wind turbine and a battery bank. In particular, the study led to the definition of an optimization strategy for the definition of the most effective energy mix under the “zero load rejection” principle, based on a long-term energy production cost analysis.

The specific contribution of the present study with respect to the previous one, and to the relevant literature, is to show the effect on the final selection of the best mix of renewable energy sources of the characteristics of the commercial that are about to be used in a real application. In many published studies up to know, beyond the specific method or model used to schematize the system and its performance, the huge number of cases to be tested in the optimization analyses in fact led the authors to treat the variables used in describing the system (e.g. nominal power outputs of the different energy source and/or physical dimensions of the same) like continuous ones. The optimization strategy was then free to adjust their values to find the optimal energy mix, even though the configuration was not always exactly reproducible with real machines available in the market. Moreover, in defining them as continuous variables, some additional assumptions may be needed. For example, in [39] a procedure was proposed to define a

generalized power curve of a wind turbine by averaging performance data of different commercial turbines of various sizes. By doing so, however, approximations are necessarily introduced.

The goal fixed by the authors in the present study is then to assess the impact on the best energy mix selection of dealing with real devices and machines, i.e. a discrete and finite number of PV panels and commercial wind turbines having given nominal power outputs and performance curves. By doing so, the results are thought to more effectively represent the scenario of a real-life application, then providing more useful information for the installation of such a system. In particular, the influence of the real wind turbine power curve in relationship to its nominal efficiency is investigated in details in the study, together with the optimal number of PV panels needed once the turbine itself has been selected. Both analyses are also repeated in case an accumulation system is provided. The results confirmed that the configurations highlighted by a conventional optimization system can be notably modified by an approach based on real components' data.

The paper is structured as follows. Section 2 presents the case study used for the analysis including the energy demand profile and the meteorological data of the site. Section 3 explains the modeling scheme of the system and highlights the main energy fluxes between the components. The characteristics of the system components, including sizes, chosen technology and efficiencies are then presented in Section 4, while Section 5 explains the assumptions and the modeling strategy based on the maximization of the economic long term savings. The results of the analysis, either including or not a battery accumulation system, are reported in Section 6. Section 7 finally draws some conclusions and future development of the study.

## 2. Case study

### 2.1 Energy consumption

The selected case study was inspired to a typical mountain chalet located in the Italian Alps, already investigated in [39]. As a reference of the electrical energy consumption, the daily load profile described in [40] was considered. This daily load profile (Fig. 1), which, in absence of further details, was considered constant throughout the year in the present analysis, is characterized by a high electricity demand (due to the chalet's facilities, the restaurant's kitchen and the guest rooms), with three marked peaks and a maximum absorption of about 20 kW. As a baseline configuration (i.e. with no renewable energy sources), this load was considered as satisfied by means of a diesel generator with a nominal power of 21 kW [40]. In order to provide an overview of the global energy demand, Tab. 1 reports the aggregated energy consumptions of the baseline configuration.

### 2.2 Meteorological data

In order to estimate the optimal sizing of the wind turbine and the PV panels stack, a set of meteorological data was firstly defined by taking into account a reference location located in the North of Italy (mountain region). More specifically, the solar irradiation data was estimated by using PVGIS (Photovoltaic Geographical Information System) [41], which is able to provide the photovoltaic potential accounting for both temperature and turbidity. The solar irradiance of the site, acquired every 10 minutes, is presented in Fig. 2.

As for the wind data, historical wind speed measurements (sampled every 10 minutes) were available thanks to a dedicated anemometric campaign carried out by the authors in partnership with a wind turbine installer (additional details cannot be reported here for confidentiality reasons) in an area close to the reference location and was considered as significant of the local wind conditions. As a further analysis, the calculated Weibull distribution (reported in Fig. 3) was compared to that obtained by using the average wind speed of the site taken from the wind atlas of RSE (Italy) [42] and a shape parameter of 1.4 (typical of mountain areas) with good agreement.

## 3. System modeling

A simplified scheme of the hybrid energy system and its energy fluxes is reported in Fig. 4. The final energy user is fed by the hybrid system whose main components are:

- A stack of PV panels
- A horizontal-axis wind turbine
- A diesel generator, having a nominal power able to satisfy even the peak load
- A bank of lead-acid batteries for energy accumulation

The energy fluxes within the system have been modeled with a "zero load rejection" principle, basically aimed at maximizing the use of renewables when available. The algorithm describing the functioning of the hybrid system is schematized in Fig. 5.

The control algorithm for the management of energy within the system was derived by the one presented in [39]. For completeness, the logical sequence of the algorithm can be summarized as follows:

- Renewables have a nominal power $P_{PVnom}$ and $P_{Wnom}$ for the photovoltaic panels and the wind turbine, respectively, according to the number of PV panels or the wind turbine that are selected in the design phase. For each source, an efficiency of energy conversion is also known as a function of the solar irradiance and temperature (for PV panels) or the wind speed (for the wind turbine). Based on the instantaneous meteorological conditions in the site (i.e. solar irradiance, temperature and wind speed) attended every 10 minutes during the year, the actual power produced by renewable sources is first calculated;
- The power contribution of the renewable energy sources ($P_{REN}$) is then compared with the actual user's energy demand ($P_{USER}$) in the same instant. A linear interpolation of the user power request was performed to match the different timing between the meteorological data (every 10 minutes) and the user request (every 30 minutes).
- In the first scenario, i.e. if an energy surplus occurs ($P_{REN} > P_{USER}$), this exceeding energy is stored into the batteries bank if not yet fully charged ($Q_{MAX}$ in Fig. 5) represents the maximum charge capacity of the accumulation system). Otherwise, the energy is necessarily dissipated.
- In a second scenario, i.e. if an energy deficit occurs ($P_{REN} < P_{USER}$) the energy accumulated in the batteries is primarily used to cover this deficit until the charge of the accumulation system reaches the discharge threshold ($Q > Q_{MIN}$). Beyond that condition, the diesel generation is activated to satisfy the energy demand.

## 4. Selected systems components

One of the key elements of the present study is represented by the fact that real machines and components are considered in the optimization analysis of the hybrid energy system. For this reason, much attention has been paid to the selection of data and characteristics of all the components.

### 4.1 PV panels

An available area exposed to the south direction and equal to 150 m$^2$ was considered for the calculation of the maximum number of panels that could be installed, since it approximately corresponds to the favourably-exposed portion of the chalet roof. Indeed, as a rooftop installation was considered, a panel inclination of 18° was taken into account (i.e. the typical roof inclination in northern Italy).

#### *4.1.1 Selected panels*

A technical and market survey was preliminary carried out in order to select a PV panel technology suitable for the present application and ensuring a good price/quality ratio (e.g. [43-45]). On this basis, the polycrystalline silicon technology was identified as the most promising. More specifically, the SOLAR FABRIK PREMIUM L POLY 250 panel was finally selected [46], having the main following characteristics:

- Nominal power for single panel $P_{PV\_S}$ = 250 W
- Nominal efficiency $\eta_{nom}$ = 15%
- Dimensions [mm]: 998 x 1667 x 35
- Area $A_{PV\_S}$ = 1.644 m$^2$ (60 cells per module)

The customer cost of this specific panel in Italy was assessed through a market analysis in August 2015 (e.g. [47]), equal to 0.62 €/W, for a global amount of 155 € per module. This cost represented the sell price of the panel only and was then quite far from the turnkey price of the system ($IC_{PV}$), which was reconstructed after a further market analysis of the installation cost. Based on an available survey specifically referred to installations in Italy [48], the different components of the final price are reported in Tab. 2, leading to a total turnkey price of $IC_{PV}$ = 2220 €/kW.

#### *4.1.2 PV panels modeling*

The power coming from PV panels was calculated with the model developed by Suri et al. [49] to create the online database PVGIS. In the model, the actual power of the panels depends on the irradiance and the real module efficiency, which is a function of the irradiance and the module temperature (Eq. 1):

$$P_{PV}(t) = GA\eta(G,T_m) = GA\eta_{nom}\eta_{rel}(G,T_m) \quad (1)$$

where $G$ is the irradiance, $A$ the area of the PV modules and η the actual module efficiency. This efficiency can be expressed as the product of the nominal efficiency $\eta_{nom}$ (declared by the manufacturer) and the relative efficiency $\eta_{rel}$, depending on the irradiance and the module temperature. The nominal efficiency $\eta_{nom}$ is calculated for a nominal irradiance of 1000 W/m$^2$ and a module temperature of 25°C.

The nominal power of the photovoltaic system can be then expressed by Eq. 2:

$$P_{PVnom} = 1000 \cdot A\,\eta_{nom} \tag{2}$$

Coupling Eq. 1 and Eq. 2, the actual power can be written as in Eq. 3:

$$P_{PV}(t) = G \cdot \frac{P_{PVnom}}{1000} \cdot \eta_{rel}(G, T_m) \tag{3}$$

i.e. the actual power $P_{PV}$ can be calculated at each instant when the irradiance of the site, the peak power of the photovoltaic system and the relative efficiency of the panels are known.

In the preliminary study reported in [39], the area of the PV panels stack $A$ was considered as a continuous variable, i.e. the panels were hypothetically assimilated to a virtual single panel of variable area. In the present study, conversely, the use of real commercial panels made the area a discrete variable, function of the number of panels $N_{PV}$ and their individual area $A_{PV\_S}$. The global power coming from PV panels was then given by Eq. 4, where $P_{PV\_S}$ is the nominal power of each panel.

$$P_{PVnom} = N_{PV} \cdot P_{PV\_S} \tag{4}$$

### 4.2 Wind turbine

*4.2.1 Turbines' selection*

A detailed market survey was also carried out for the identification of proper wind turbines, among which one could choose the one to be installed. Based on previous results of [39], a range of nominal power between 1 and 25 kW was *a priori* imposed in the survey; moreover, for every considered rotor, the power curve declared by the manufacturer was accurately checked, discarding all those cases in which power coefficient values were higher than the standards or unconventional cut-in and cut-off limits were indicated. On these bases, 12 turbines were finally selected, having rated power values between 1.4 and 25 kW [50-61]. Figure 6 resumes the power curves of selected rotors; for the sake of simplicity, a constant cut-off wind speed of 25 m/s was imposed to all turbines as it is apparent by looking at Fig. 3 that wind speeds over this velocity rarely occur. All the turbines were supposed as installed at the same height above the ground, equal to 25 m (the largest turbine considered has a diameter of 10 m [61]).

*4.2.2 Installation cost*

The installation cost of small and medium-size wind turbines is somehow a controversial issue, since it is not always declared or easily arguable from published data. Based on a literature survey (e.g. [17-18]) and on the authors' experience, a reference value of approximately 5000 €/kW can be suggested. This value is reasonably accurate for wind turbines up to nominal power outputs of 5 kW, while it can be substantially reduced when the size of the turbine increases [62]. For the purpose of the present study, a cost function, reported in Fig. 7 has been hypothesized based on data (empty dots in the figure) coming from the literature survey of [62] and from personal installation experience of the authors.

### 4.3 Diesel generator

Based on the peak energy consumption of the chalet, the selected diesel generator was the Perkins 404D-22G [63], having a nominal power of 21.3 $kW_e$. The power-consumption curve was derived from [63] (Fig. 8) and used to estimate the consumption of the engine in different operational conditions. For load values less than 50%, the minimum value of 263 g/kWh was considered. A life time of 25000 hours was finally considered for the diesel generator [39].

Finally, the installation cost was estimated from the official catalog of the producer ($IC_{DG}$ = 5800 €), corresponding to a specific cost of 276 €/kW. This value was in line with the indication of a web-based market survey carried out on August 2015 for the Italian market.

### 4.4 Batteries

A lead acid battery bank was selected as energy storage. Selected batteries had an output voltage of 48 V, whereas a sensitivity analysis on battery capacity was carried out. In further detail, lead acid batteries were indeed selected since they ensure high reliability, low auto-consumption, good stability and an excellent cyclic behavior, particularly important for stand-alone applications [64]. Since it was not easy to estimate the lifetime in discharging cycles for the present application (the batteries indeed are expect to undergo many partial-discharging phases), an estimated lifetime of 61000 hours was considered, after which they must be replaced.

## 5. Economic model and optimization strategy

### 5.1 Economic model of the system

The economic model of the system, used in the optimization process to define the convenience of each solution, was built in accordance to the one proposed in [17], even if improvements were provided in the modeling of the wind

turbine cost function and in the modeling of maintenance costs. For the sake of completeness, the basic elements of the model are here presented and explained; for additional details please refer to [17].

The final goal of the economic model was the definition of the *long term savings (LTS)* for each design solution of the hybrid system. This was done by comparing the long term cost of the hybrid system (*CN*) to the expected costs deriving from the use of the diesel generator only (i.e. the baseline configuration). As in all complete economic analyses, the long term cost in an *n*-years' time horizon has to account for the capital cost of the installed equipment *($IC_0$)* and the maintenance and operation costs of the same, that can be further divided into a fixed component ($FC_n$) and a variable component ($VC_n$).

The installation cost $IC_0$ is given by the sum of the market cost of the different component at year 0. In the present model, it is defined by Eq. 5, where proper cost functions for the market costs are introduced.

$$IC_0 = \alpha P_{PVnom} + f_1(P_{Wnom}) + P_{DG} \cdot \gamma + \lambda \cdot P_{USERpk}^{(1-\tau)} + b \cdot P_{RINnom} + \xi \cdot Q_{\max}^{(1-\omega)} \tag{5}$$

More in details, parameters $\alpha$ and $\gamma$ are the specific installation costs, in €/kW, of the PV panels and the diesel generator, respectively. Parameters $\lambda$ [€/kW], $\tau$ and $b$ [*€/kW*] instead refer to installation costs of the electronic devices and then depend on the magnitude of the peak load and the total nominal power of renewables. Finally, factors $\xi$ [€/Ah] and $\omega$ [cost.] describe the battery bank purchase costs, as reported in [39].

Function $f_1$ is the complex cost function for the wind turbine described in Section 4.2.2 (Eq. 6).

$$IC_W = 4.6632 P_{Wnom}^2 - 247.29 P_{Wnom} + 6169.9 \tag{6}$$

The fixed maintenance and operation costs are instead described by Eq. 7:

$$FC_n = m \cdot IC_0 \cdot (1+g_m) \cdot (1+i)^n \cdot \frac{\left[1 - \frac{(1+g_m)^n}{(1+i)^n}\right]}{(i-g_m)} + c_f \cdot M_f \cdot (1+e_f) \cdot (1+i)^n \cdot \frac{\left[1 - \frac{(1+e_f)^n}{(1+i)^n}\right]}{(i-e_f)} \tag{7}$$

Factor $m$ represents the maintenance and operation costs, expressed as a fraction of the installation cost of the system components, while, as prescribed by [65], factor $g_m$ is the annual inflation rate, accounting for the annual changes in labor cost and spare part costs. In the formulation of Eq. 7, the fuel consumption cost is also considered, depending on the current fuel price $c_f$, the annual fuel consumption $M_f$ and the oil price escalation rate $e_f$.

The variable maintenance and operation costs are finally given by Eq. 8, where $VC_{DG}$ and $VC_{BAT}$ are the variable maintenance costs of the diesel generator and the battery bank, respectively.

$$VC_n = VC_{DG} + VC_{BAT} \tag{8}$$

These costs have a discontinuous nature, i.e. they are introduced in the economic model of the system only when the lifetime of components is reached. On these bases, in the present model they were considered as described by Eqs. 9 and 10, respectively, where $h_{DG}$ and $h_{BAT}$ are the diesel generator and batteries operational hours, $life_{DG}$ and $life_{BAT}$ the estimated diesel generator and battery bank lifetime, both considered for simplicity in hours. After the lifetime of the components is reached, the cost connected to their new buy is introduced in the model.

$$VC_{DG} = 0 \; if \; h_{DG} \neq life_{DG} \quad \text{otherwise} \quad VC_{DG} = IC_{DG}\left(\frac{1+g_m}{1+i}\right)^{(hDG/8760)} \tag{9}$$

$$VC_{BAT} = 0 \; if \; h_{BAT} \neq life_{BAT} \quad \text{otherwise} \quad VC_{BAT} = IC_{BAT} \cdot \left(\frac{1+g_m}{1+i}\right)^{(hBAT/8760)} \tag{10}$$

The selected parameters for the economic analysis are finally summarized in Tab. 3 [4, 48].

### 5.2 Strategy and goals of the optimization

As discussed, the goal of the optimization was the definition of the best energy mix for the hybrid system, based on the maximization of the long terms savings in a 10-years period in comparison to the original solution with the diesel generator only. This timeline was chosen more on an economic basis than on an end-of-life reference. In [39], some of the authors carried out the same analysis not accounting for real machines, but treating the nominal power values of the PV panels and the wind turbine as continuous variables. This solution will be considered also in the present study for comparison purposes and will be referred to as "Case 1". In this approach, the wind power will be managed using a reference power curve which was obtained by dividing the wind turbine curves for their relative peak power (i.e. $P/P_{nom}$) and calculating an average trend (see Fig. 9). By doing so, the reference curve can be considered somehow representative of the selected rotors, being also able to partially discard some peculiar trends like those of the stall controlled Montana 5.6 and Excel 7.5, or the strange peak power of the Antaris 9.5. Overall, it can be noticed that the reference curve is quite similar to at least four curves, corroborating the effectiveness of present assumptions.

As a further analysis, in this study real machines are now considered. As a result, the rated power of PV panels is now a function of the number of selected modules, whereas the power of the wind turbine is directly dependent on the machine considered in each case. This new configuration will be referred to as "Case 2" in the continuation of the work. In comparison to previous studies where real turbine data was considered (e.g. [66]), the focus of the research was the identification of the energy mix (number of PV panels and wind turbine) that guarantees the highest long term saving.

### 5.3 Optimization software

The described model of the system (Fig. 5) was implemented in MATLAB®. The optimization process was performed by using ModeFrontier® with a design of experiments based on a Sobol pseudo random sequence. The experiments were uniformly distributed between the minimum and maximum values assigned to the input variables. The optimization method was the genetic algorithm Multi Objective Genetic Algorithm (MOGA-II) that was performed for 50 generations and a DNA mutation ratio of 0.05.

As a reference value, the combination Sobol/MOGA-II analyzed with these settings leads to a total of 1000 design for each run in Case 1. The input variables of the optimization in Case 1 were the nominal wind and solar powers, which were varied from 0 to 25 and 15 kW, respectively. The variation steps were 0.1 kW for the wind power and 0.5 kW for the solar power. In Case 2, conversely, the input parameters were the number of PV panels $N_{PV}$ and the wind turbine selected, with its rated power $P_{Wnom}$.

## 6. Results and discussion

All the results presented in the study will be evaluated in comparison to the baseline solution, in which the entire energy demand of the user is covered by the diesel generator. According to the selected generator [63], the annual fuel consumption in these conditions is equal to 9434 l/year, whereas the overall cost of the system $CN_{DG}$ over 10 years is equal to 351.430 € (including initial costs, fuel consumption and maintenance).

### 6.1 Case 1 - no battery

The analysis of Case 1 results, with no storage system, is of particular interest to understand the quantitative response of the system and was considered very useful for the rest of the analysis. This case study, in fact, allows one to estimate the influence of photovoltaic or wind systems and the difference between solutions with the same rated powers. In particular, Fig. 10 reports the point cloud of all systems feasible solutions (LTS > 0) with given constraints. In the figure, the different solutions have been reported in a blue color scale in order to stress the influence of the photovoltaic power $P_{PV}$. The left boundary of the cloud, ensuring the maximum long-term savings, corresponds to the maximum allowed photovoltaic power of 15 kW and is highlighted with yellow-filled marks.

Upon examination of the figure, it is apparent that, as far as the installed photovoltaic power is reduced, the curves are shifted towards the upper left corner of the solution space, i.e. towards higher fuel consumptions and lower LTS, since the use of the diesel generator is progressively increased. According to previous results of [39], it is here confirmed that moving on the top limit of the cloud (from right to left), the configurations are characterized by a decreasing $P_{Wnom}$ value, the diesel consumption grows in this direction, as the internal combustion engine usage increases, whereas the long term cost decreases due to the increasing cost of needed fuel. In the lower limit of the cloud, conversely, moving from the vertex to bottom left, the points are characterized by an increasing wind turbine nominal power. In this case, the annual diesel consumption decreases because the wind turbine is able to cover a greater portion of the load profile. The long term cost, however, decreases due to the higher costs of installation and maintenance of the turbine. In Fig. 10 some other relevant solutions at fixed wind power are also highlighted with a red color-scale, corresponding to rated power outputs of 12.5, 20 and 25 kW. As one can notice, in each of these curves, the point having the maximum LTS lies in the left boundary of the paraboloid, i.e. where the photovoltaic power is maximum. This result confirms that the PV panels appear as the most convenient solution for this specific application. Moreover, it is worth pointing out that the maximum LTS is not monotonic with the installed wind power, i.e. an optimum wind power value does exist, able to maximize the LTS in correspondence to the maximum PV power.

To assess this observation, Fig. 11 describes how the nominal power of the wind turbine influences the system savings (in case the maximum PV power is installed). In the first part of the graph, the long term saving increases, reaching his maximum for a value of $P_{Wnom}$=20 kW (empty mark in the figure), and then decreases again. As discussed, after the peak the economic benefits coming from fuel savings are no longer able to counterpart the increased installation and maintenance costs of the turbine.

### 6.2 Case 2 - no battery

Moving now to the analysis of real-machines effects (again not accounting for an accumulation system), Fig. 12 reports the feasible solutions in Case 2: as discussed, the wind power is now dependent on the specific turbine that is selected, i.e. it is not represented anymore by a continuous variable. Moreover, in each curve, the PV power is now a direct function of the number of installed panels.

According to the results in Case 1, the right margin of each curve is characterized by a maximized photovoltaic power. The progressive increase of $N_{PV}$ in each curve induces a notable decrease of fuel consumption and an increase of LTS, thanks to the discussed suitability of solar power for the present application. The influence of PV panels' number is almost constant for all wind turbines, i.e. the different curves are almost parallel. Upon examination of the cloud, it is also apparent that the same LTS can be achieved in several cases with different ratios between solar and wind power.

The point at the extreme right of the cloud still represents the system configuration having the maximum LTS (68.223,00 €), now corresponding to the maximum number of PV panels ($N_{PV}$ = 60), i.e. $P_{PVnom}$=15 kW, and the wind turbine having a rated power of $P_{Wnom}$=12 kW. This latter result is of particular interest since it differs from the optimal configuration in Case 1. In detail, if it is indeed true that larger wind turbines ensure very low fuel consumptions, in the present case the increase of installation cost, combined with the specific power coefficient curve of each rotor, makes a smaller wind turbine more convenient from an economic point of view, even if a larger use of the diesel generator is attended. This trend is also testified by Fig. 13, which reports the long-term savings of all solutions (different turbines are again displayed with dedicated marks) with $N_{PV}$ = 60 (right boundaries of all curves) as a function of the nominal wind power. Upon examination of the figure, it is again confirmed that, in general, higher LTS can be achieved in the right side of the solution space, i.e. for higher installed wind power. However, the use of real machines induces a "scatter" in the results, making different solutions more convenient due to more favorable combination between installation cost and efficiency.

### 6.3 Comparative performance analysis between Case 1 and Case 2

In Sections 6.1 and 6.2 the optimal energy mix for the analyzed system with no accumulation has been defined in Case 1 and Case 2, respectively. Some additional remarks can be done by comparing the performance of these configurations in the selected time-horizon of 10 years. To do so, Fig. 14 compares the installed power values for PV panels and the wind turbine in the two cases with the energy really harvested by the same; Fig. 15 instead compares the economic performance of the two systems.

Upon examination of Fig. 14, one can readily notice that the installation of a smaller wind turbine (-37.5% rated power) in Case 2 obviously leads to a reduction of harvested energy (-26.2%). However, due to a more rational exploitation of energy fluxes, the total dissipated energy is reduced by -27.5%. Focusing on Fig. 15, it is also apparent that the lower fuel saving in Case 2 is compensated by a notably lower installation cost of the system (due to the smaller wind turbine), which finally induce a LTS higher than in Case 1 by 12.3%.

Discussed differences are significant of the potential impact of real machines on the optimization process of similar systems. In particular, since the function for the wind turbine installation cost is the same in Case 1 and Case 2 and optimal system configurations in the two cases always implies a maximum PV panels power, it should be attended the approximately the same optimal configuration is about to be obtained. However, the use of the specific power curve for the wind turbine instead of a reference curve induces a notable difference in the expected wind energy harvesting, leading to a different energy mix. To further analyze these aspects, the optimal solution of Case 2 was compared in Tab. 4 with that having $P_{Wnom}$=20kW, i.e. the same optimal wind power expected by Case 1 analysis; as testified by Fig. 13, this configuration is in fact the second one in terms of LTS.

Upon examination of the results, it is again apparent that the biggest difference is given by the relative increase of harvested energy due to the higher efficiency of the smaller turbine, which is able to compensate the higher fuel consumption and the proportionally higher installation cost of the turbine itself (see Fig. 8). Overall, the results demonstrate that the considered power curve of the selected wind turbine can have a major impact on the optimization analysis and then it is worth of accurate evaluation in similar studies.

### 6.4 Sensitivity analysis on PV power

An accurate analysis of Fig. 12 leads to the consideration that none of the curves presented a parabolic trend in Case 2, which was however commonly seen in Case 1 (see Fig. 10). Since the optimal system configuration generally implies the highest available PV power, it was argued that the use of real machines/devices in Case 2 could benefit from a larger installed photovoltaic power. Of course, the following analysis somehow lies outside the proposed system, in which the area available for PV panels was limited to 150 $m^2$; however, the analysis of optimal configurations in Case 2 is of particular interest to further discuss the impact of real machines on the optimal energy mix. To this purpose, the analysis of section 6.2 was repeated with a doubled available number of PV panels, i.e. $N_{PV}$=120. Under these preconditions, the new feasible system configurations are reported in Fig. 16.

Results of Fig. 16 are indeed of particular interest. Sweeping the curves from left to right, the final point of each curves represents the configuration with the maximum number of PV panels, i.e. $N_{PV}$=120. As a result, for the selected wind turbine, this configuration is the one with the lowest annual fuel consumption, since the use of renewables is maximized. It is also apparent, however, that for some curves (i.e. wind turbine selections), this configuration is also the one in fact giving the highest LTS, like in Case 1, whereas a different optimal configuration is achieved in many other cases. In these latter configurations, the increase of PV installation cost makes additional panels not convenient in comparison to the energy amount already harvested by means of the wind turbine. The discussed results are more effectively shown in Fig. 17, which reports the optimal number of PV panels ($N_{PV}$) as a function of the selected nominal wind power in Case 2. Upon examination of the figure, it is apparent that only four turbines (i.e. the ones with the lower

nominal power rates) lead to the use of the maximum number of panels available, whereas a quadratic decrease of $N_{PV}$ as a function of the nominal power is evident. In the same figure, the long-term savings of the different configurations is also reported, clearly showing that the largest savings are not obtained in correspondence to the largest installed power from renewables, but again for a medium-size, very efficient turbine ($P_{Wnom}$=12 kW) and a number of PV panels $N_{PV}$=97. This latter value was indeed lower than the limit of 120, but higher than the original limit of 60 accounted for in the Case 1 analysis.

### 6.5 Effects of the storage system

The analysis of Case 1 and Case 2 configurations without energy accumulation is of specific interest to understand the physics of the system and the relative impact of each energy source. In a real-life design of such a complex hybrid system, however, the presence of a storage system is mandatory to rationalize the energy fluxes. In the present study, a sensitivity analysis on the battery capacity was then carried out with nominal batteries capacity ranging from 250 Ah to 2250 Ah (the preliminary study reported in [39] indeed indicated a reference capacity of $Q_{max}$=1500 Ah).

First, the impact of an energy accumulation on the performance of the energy system was assessed in the three relevant cases analyzed so far, i.e. Case 1 (Fig. 18), Case 2 (Fig. 19) and Case 2b (Fig. 20), which represents the Case 2 approach with a maximum number of PV panels sufficient to identify the unconstrained optimal energy configuration. In all cases, new solutions are compared to the optimal ones without accumulation (light-grey clouds).

Upon examination of the results, it is apparent that in all the optimization strategies, the introduction of an accumulation system provides great benefits in terms of reduction of fuel consumption and increase of the long term savings, which were more than doubled with respect to previous analyses. In further detail, in case of continuous-variable optimization (Case 1 - Fig. 18) the maximum LTS was increased by 110%, in case of real wind turbine curves (Case 2 - Fig. 19) by approximately 90%, while in case of unconstrained $N_{PV}$ (Case 2b - Fig. 20) again by approximately 90%. This result is in line with the former results of [39] and with the relevant technical literature (e.g. [18] or [20]).

Once the benefits of accumulation have been assessed, a sensitivity analysis on the battery capacity was carried out in both optimization strategies. The most relevant results of this analysis are reported in Fig. 21, where the parameters of the optimal solutions (i.e. the vertices of the solutions clouds of Fig. 18 and Fig. 19) are reported as a function of the battery capacity in Case 1 and Case 2 (analogous trends than Case 2 were indeed obtained for Case 2b). The results clearly showed that the performance of the energy system is monotonically increased by a superior capacity of the accumulation system. In both optimization strategies, however, the trends flatten in correspondence to the highest capacity tested ($Q_{max}$=2250 Ah), corresponding to the condition in which the increased cost of a larger accumulation system does not provide any more sufficient savings coming from a reduced dissipation of renewables.

Finally, in order to understand more in details the impact of the accumulation system on the system configuration, Tab. 5 compares the optimal energy mixes in Case 2 for the four analyzed battery pack capacities.

Beyond the discussed monotonic increase of the LTS with the batteries capacity, Tab. 5 provides a very interesting insight on the effect of the accumulation system. In further detail, it is worth remarking that the introduction of the accumulation did not alter the optimal sizing of renewables, i.e. $P_{PVnom}$ and $P_{Wnom}$ are always the ones found in the analysis of Case 2 with no batteries.

This result is indeed of particular relevance, since it could be expected that the presence of an accumulation system should have led to the selection of smaller machines, with a consequent reduction of the capital cost of the system. Conversely, Tab. 5 clearly shows that the increase of LTS is only connected to the reduction of dissipated energy coming from renewable source through a more rational management of energy fluxes. By doing so, the use of the diesel generator to compensate peak loads can be substantially reduced, with notable money savings, by far higher than the increases in the capital cost of the batteries themselves.

### 6.6 Daily load profiles analysis

The impact on the accumulation system, discussed in Section 6.5, is even more evident if one analyzes the daily coverage of the user demand with the different system configurations. For example, Fig. 22 reports the comparison of daily profiles coverage for June 21$^{st}$ of optimized systems in Case 2 with or without the accumulation system ($Q_{max}$ = 1500 Ah). Upon examination of the comparison, one can readily notice that the power coming from renewables is now more rationally exploited in case of the system with the battery bank, with a reduction of the energy from renewables that is dissipated of more than 96%. This power is now used either to satisfy the user demand or to re-charge the batteries. In particular, it is worth noticing that, for this specific day of the year and system configuration, the battery is able to completely replacing the diesel generator, simply making use of energy surplus coming from renewable sources.

## 7. Conclusions

In the study, a sizing strategy, based on a long-term energy production cost analysis, was used to assess the optimum configuration of a hybrid PV-wind-diesel stand-alone system, representing an isolated mountain chalet in Italian Alps.

In particular, the results of a conventional optimization strategy, threating rated power values of renewable source as continuous variables to create the available design space, were compared to those of a strategy making use of real machines data and realistic constraints.

Results first showed that, in case the real characteristics of commercial PV panels and wind turbines are considered, the optimal energy mix for the system is changed. In detail, it was found that if it is indeed true that larger wind turbines ensure very low fuel consumptions, in the present case the increase of installation cost, combined with the specific power coefficient curve of each rotor, made a smaller wind turbine (12 kW vs. 15 kW) more convenient from an economic point of view, even if a larger use of the diesel generator is attended.

Depending on the site, it was also noticed that the effective wind turbine power curve can have a major impact on the sizing of the system. More in detail, it was observed that, even if the PV panels were in general the more convenient source included in the system, an optimal panel number can be anyhow identified for the system, once the wind turbine was selected, in correspondence to the point in which the higher installation cost is not anymore compensated by the reduction of fuel consumption. For the specific case study, where the installation available area only allowed a number of panels equal to 120, this limit was reached as the best compromise only for the four wind turbines with the lower rated power outputs. For higher wind capacities, the optimal number of PV panels was progressively reduced of more than 35%.

The capacity of the battery pack did not alter the optimal energy mix previously identified for renewables without accounting for accumulation, since the primary convenience of batteries was the minimization of the use of diesel generator during the year and not the replacement of renewables in satisfying the energy demand of the user. Notwithstanding the above, the use of a properly sized battery pack can notably rationalize the exploitation (and hence the convenience) of renewables. As an example, for the considered site the best configuration with a battery pack of 1500 Ah was able to ensure a reduction of the dissipated power from renewables during the day up to more than 110%.

Given the present interest in similar applications, the present study demonstrates once more that the identification of realistic data prior to undertaking the optimization of small hybrid energy systems is essential to identify really feasible solutions and is then a mandatory requirement for designers facing real-life applications.

## References


[1] International Renewable Energy Agency (IRENA). Off-grid renewable energy systems: status and methodological issues, http://www.irena.org/DocumentDownloads/Publications/IRENA_Off-grid_Renewable_Systems_WP_2015.pdf ; 2015 [accessed 04.04.16].

[2] Bloomberg New Energy Finance. Off-grid solar market trends report 2016, http://about.bnef.com/white-papers/off-grid-solar-market-trends-report-2016/ ; 2016 [accessed 04.04.16].

[3] Wind energy - The facts, www.wind-energy-the-facts.org ; 2009 [accessed 04.04.16].

[4] Kaldellis JK. Optimum autonomous wind–power system sizing for remote consumers, using long-term wind speed data. Applied Energy 2002;71:215-18. DOI: 10.1016/S0306-2619(02)00005-3

[5] Narula, S.A., Bhattacharyya, S., 2017. Off-grid electricity interventions for cleaner livelihoods: A case study of value chain development in Dhenkanal district of Odisha. J. of Cleaner Production 142 (Part 1, 20 January 2017), 191-202. DOI: 10.1016/j.jclepro.2016.07.176

[6] Chowdhury, S.A., Aziz, S., Groh, S., Kirchhoff, H., Filho, W.L, 2015. Off-grid rural area electrification through solar-diesel hybrid minigrids in Bangladesh: resource-efficient design principles in practice. J. of Cleaner Production 95 (15 May 2015), 194-202. DOI: 10.1016/j.jclepro.2015.02.062

[7] Shezan, SK.A., Julai, S., Kibria, M.A., Ullah, K.R., Saidur, R., Chong, W.T., Akikur, R.K., 2016. Performance analysis of an off-grid wind-PV (photovoltaic)-diesel-battery hybrid energy system feasible for remote areas. J. of Cleaner Production;125(1 July 2016):121-132. DOI: 10.1016/j.jclepro.2016.03.014

[8] Bigerna, S., Bollino, C.A., Micheli, S., 2016. Socio-economic acceptability for smart grid development - a comprehensive review. J. of Cleaner Production;131(May 2016):399-409.

[9] Cardenas J.A., Gemoets, L., Ablanedo Rosas J.H., Sarfi, R., 2014. A literature survey on Smart Grid distribution: an analytical approach. J. of Cleaner Production;65(October 2014):202-216.

[10] Boroojeni, K.G., Hadi Amini, M., Nejadpak, A., Dragicevic, F., Iyengar, S.S., Blaabjerg, F., 2016. A Novel Cloud-based Platform for Implementation of Oblivious Power Routing for Clusters of Microgrids. IEEE Access, http://dx.doi.org/10.1109/ACCESS.2016.2646418

[11] Boroojeni, K.G., Hadi Amini, M., Nejadpak, A., Iyengar, S.S., Hoseinzadeh, B., Leth Bak, C., 2016. A theoretical bilevel control scheme for power networks with large-scale penetration of distributed renewable resources. Electro Information Technology (EIT), 2016 IEEE International Conference on IEEE, 2016

[12] Hadi Amini, M., Moghaddam, M.P., Karabasoglua, O., 2017. Simultaneous allocation of electric vehicles' parking lots and distributed renewable resources in smart power distribution networks. Sustainable Cities and Society;28: 332-342

[13] Hadi Amini, M., Nabi, B., Haghifam, M.-R., 2013. Load management using multi-agent systems in smart distribution network. IEEE PES General Meeting, Vancouver, BC, Canada, 2013

[14] International Energy Agency. Africa Energy Outlook - World Energy Outlook Special Report, https://www.iea.org/publications/freepublications/publication/WEO2014_AfricaEnergyOutlook.pdf ; 2014 [accessed 04.04.16].
[15] Li, C., Yu, W., 2016. Techno-economic comparative analysis of off-grid hybrid photovoltaic/diesel/battery and photovoltaic/battery power systems for a household in Urumqi, China. J. of Cleaner Production 124 (15 June 2016), 258-265. DOI: 10.1016/j.jclepro.2016.03.002
[16] Hemmati, R., 2017. Technical and economic analysis of home energy management system incorporating small-scale wind turbine and battery energy storage system. J. of Cleaner Production;159 (May 2017):106-118. DOI: 10.1016/j.jclepro.2017.04.174
[17] Kaldellis JK, Zafirakis D, Kavadias K, Kondili E. Optimum PV-diesel hybrid system for remote consumers of the Greek territory. Applied Energy 2012;97:61-66. DOI: 10.1016/j.apenergy.2011.12.010
[18] Kaldellis JK, Zafirakis D, Kaldelli EL, Kavadias K. Cost benefit analysis of a photovoltaic-energy storage electrification solution for remote islands. Renewable Energy 2009;34:1299–311. DOI: 10.1016/j.renene.2008.09.014
[19] Kaldellis JK, Vlachos GTh. Optimum sizing of an autonomous wind–diesel hybrid system for various representative wind-potential cases. Applied Energy 2006;83:113-132. DOI: 10.1016/j.apenergy.2005.01.003
[20] Kaldellis JK, Kondili E, Filios A. Sizing a hybrid wind-diesel stand-alone system on the basis of minimum long-term electricity production cost. Applied Energy 2006;83:1384-1403. DOI: 10.1016/j.apenergy.2006.01.006
[21] Chua KJ, Yang WM, Er SS, Ho CA. Sustainable energy systems for a remote island community. Applied Energy 2014;113:1752–1763. DOI: 10.1016/j.apenergy.2013.09.030
[22] Bekele G, Tadesse G. Feasibility study of small Hydro/PV/Wind hybrid system for off-grid rural electrification in Ethiopia. Applied Energy 2012;97:5-15. DOI: 10.1016/j.apenergy.2011.11.059
[23] Ismail MS, Moghavvemi M, Mahlia TMI. Design of an optimized photovoltaic and microturbine hybrid power system for a remote small community: Case study of Palestine. Energy Conversion and Management 2013;75:271-281. DOI: 10.1016/j.enconman.2013.06.019
[24] Omer ZM, Fardouna AA, Alameri AM. Economic Feasibility Study of Two Renewable Energy Systems for Remote Areas in UAE. Energy Procedia 2015;75:3027-3035. DOI: 10.1016/j.egypro.2015.07.617
[25] Proietti S, Sdringola P, Castellani F, Garinei A, Astolfi D, Piccioni E, Desideri U, Vuillermoz E. On the possible wind energy contribution for feeding a high altitude Smart Mini Grid. Energy Procedia 2015;75:1072-1079. DOI: 10.1016/j.egypro.2015.07.483
[26] Baghdadi F, Mohammedi K, Diaf S, Behar O. Feasibility study and energy conversion analysis of stand-alone hybrid renewable energy system. Energy Conversion and Management 2015;105:471-479. DOI: 10.1016/j.enconman.2015.07.051
[27] Ismail MS, Moghavvemi M, Mahlia TMI. Techno-economic analysis of an optimized photovoltaic and diesel generator hybrid power system for remote houses in a tropical climate. Energy Conversion and Management 2013;69:163-173. DOI: 10.1016/j.enconman.2013.02.005
[28] Luo Y, Shi L, Tu G. Optimal sizing and control strategy of isolated grid with wind power and energy storage system. Energy Conversion and Management 2014;80;407-415. DOI: 10.1016/j.enconman.2014.01.061
[29] Clastres, C., Ha Pham, T.T., Wurtz, F., Bacha, S., 2010. Ancillary services and optimal household energy management with photovoltaic production. Energy;35:55-64.
[30] Molderink, A., Bakker, V., Bosman, M.G.C., Hurink, J.L., Smit, G.J.M., 2009. Domestic Energy Management Methodology for Optimizing Efficiency in Smart Grids. 2009 IEEE Bucharest PowerTech, 1-7.
[31] Mets, K., Verschueren, T., Turck, F.D., Develder, C., 2011. Exploiting V2G to optimize residential energy consumption with electrical vehicle (dis)charging. In: 2011 IEEE First International Workshop on Smart Grid Modeling and Simulation (SGMS), 7-12.
[32] Leehter, Y., Wen-Chi, C., Rong-Liang, Y., 2005. An iterative deepening genetic algorithm for scheduling of direct load control. IEEE Trans. Power Syst.;20:1414-1421.
[33] Shirazi, E., Jadid, S., 2017. Cost reduction and peak shaving through domestic load shifting and DERs. Energy;124:146-159.
[34] Elkhorchani, H., Grayaa, K., 2016. Novel home energy management system using wireless communication technologies for carbon emission reduction within a smart grid. J. Clean. Prod.;135:950-962.
[35] Abdul Aziz, E., Wan Alwi, S.R., Lim, J.S., Abdul Manan, Z., Klemes, J.J., 2017. An integrated Pinch Analysis framework for low CO2 emissions industrial site planning. J. Clean. Prod.;146:125-138.
[36] Klemes, J.J., Varbanov, P.S., Kravanja, Z., 2013. Recent developments in process integration. Chem. Eng. Res. Des.;91(10):2037-2053.
[37] Kulkarni, G.N., Kedare, S.B., Bandyopadhyay, S., 2007. Determination of design space and optimization of solar water heating systems. Solar Energy;81(8):958-968.
[38] Jacob, A.S., Banerjee, R., Ghosh, P.C., 2018. Sizing of hybrid energy storage system for a PV based microgrid through design space approach. Applied Energy; 212;(15 feb 2018):640:653. DOI: 10.1016/j.apenergy.2017.12.040
[39] Bianchini A, Magnelli N, Ferrara G, Carnevale EA, Ferrari L. Optimization of a PV-wind-diesel hybrid system for a remote stand-alone application. Energy Procedia 2015;81:133-145. DOI: 10.1016/j.egypro.2015.12.068

[40] Enereco. Programma di intervento "Enereco" nei rifugi alpini, http://www.enerecosrl.com/public/files/RelazBedole.pdf ; 2013 [accessed 05.04.16].
[41] PVGIS. http://re.jrc.ec.europa.eu/pvgis ; [accessed 05.04.16].
[42] RSE. http://atlanteeolico.rse-web.it ; [accessed 05.04.16].
[43] Maycock PD. PV review. Refocus 2005;6(5):18-22. DOI: 10.1016/S1471-0846(05)70452-2
[44] Lazou AA, Papatsoris AD. Economics of photovoltaic stand-alone residential households: a case study for various European and Mediterranean locations. Solar Energy Materials and Solar Cells 2000;62(4):411-427. DOI: 10.1016/S0927-0248(00)00005-2
[45] Kaldellis JK, Doumouliakas J, Michalis K. Optimum stand-alone PV solution, including financial aspects. Proc. of the World Renewable Energy Congress VI, Brighton, UK, 2000.
[46] Solar Fabrik, http://www.solar-fabrik.de ; [accessed 05.04.16].
[47] http://www.utopiaenergy.it ; [accessed 25.08.15].
[48] http://www.fotovoltaicosulweb.it/guida/i-costi-del-fotovoltaico.html ; [accessed 25.08.15].
[49] Šúri M, Huld TA, Dunlop ED. PV-GIS: a web-based solar radiation database for the calculation of PV potential in Europe. International Journal of Sustinable Energy 2005;24:55-67. DOI: 10.1080/14786450512331329556
[50] Passaat 1.4 kW turbine - Fortis Wind Energy. http://fortiswindenergy.com/passaat/ ; [accessed 25.08.15].
[51] TI/3.6/3 turbine – Travere Industries. http://www.urbanwind.net/pdf/CATALOGUE_V2.pdf ; [accessed 25.08.15].
[52] Montana 5.6 - Fortis Wind Energy. http://fortiswindenergy.com/montana/ ; [accessed 25.08.15].
[53] Excel 6 turbine - Bergey. http://bergey.com/documents/2013/10/excel-6-swcc-summary-report.pdf ; [accessed 07.04.16].
[54] Excel 7.5 turbine - Bergey. http://bergey.com/documents/2012/03/excel-7-5-r-owners-manual.pdf ; [accessed 07.04.16].
[55] Excel 10 turbine - Bergey. http://bergey.com/documents/2013/10/excel-10-spec-sheet_2013.pdf ; [accessed 07.04.16].
[56] Antaris 6.5 - Braun. http://www.braun-windturbinen.com/products/antaris-small-wind-turbines/antaris-6-5-kw/ ; [accessed 25.08.15].
[57] Antaris 9.5 - Braun. Available: http://www.braun-windturbinen.com/products/antaris-small-wind-turbines/antaris-9-5-kw/ ; [accessed 25.08.15].
[58] SEI_RPI 12/10 turbine - Società Elettrica Italiana. http://www.societaelettricaitaliana.it/generatore_minieolico_SEI_RPI_12kW.htm ; [accessed 25.08.15].
[59] MRG 15 turbine - Morenergy. http://www.morenergysrl.it/MRG15.pdf ; [accessed 25.08.15].
[60] Westwind 20 - VG Energy. http://www.vgenergy.co.uk/files/5913/6119/8240/Westwind_Brochure.pdf ; [accessed 25.08.15].
[61] Wind Runner 25 - Eoltec. http://www.urbanwind.net/pdf/CATALOGUE_V2.pdf ; [accessed 25.08.15].
[62] Syngellakis K, Robinson P. Urban wind turbines: Development of the UK market. Proc. of the EWEC 2006, 27 February - 2 March 2006, Athens (Greece).
[63] Perkins. http://www.perkins.com/en_GB/products/new/perkins/electric-power-generation/diesel-generators/1000002596.html ; [accessed 07.04.16].
[64] Salas V, Suponthana W, Salas RA. Overview of the off-grid photovoltaic diesel batteries systems with AC loads. Applied Energy 2015;157:195-216. DOI: 10.1016/j.apenergy.2015.07.073.
[65] Kaldellis JK, Zafirakis D, Kondili E. Optimum autonomous stand-alone photovoltaic system design on the basis of energy pay back analysis. Energy 2009;34:1187-11. DOI: 10.1016/j.energy.2009.05.003
[66] Notton G., Cristofari P., Poggi P., Muselli M., Wind Hybrid Electrical Supply System: Behaviour Simulation and Sizing Optimization. Wind Energy 2001; 4:43–59 (DOI: 10.1002/we.46)

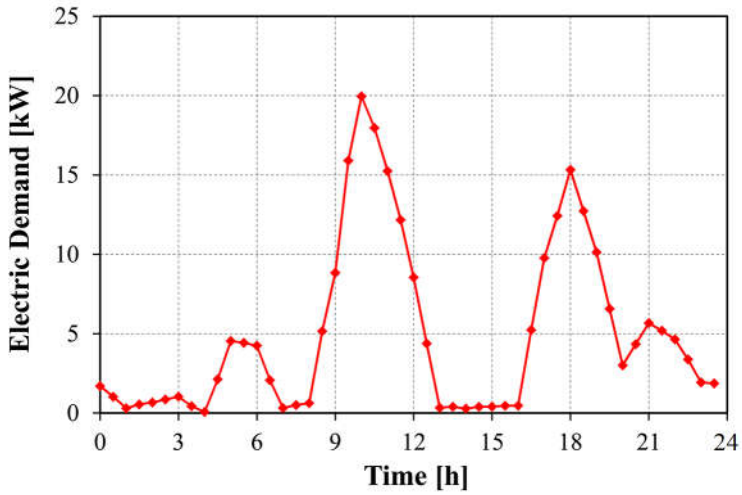
Electric Demand [kW]
Time [h]
0
5
10
15
20
25
0
3
6
9
12
15
18
21
24

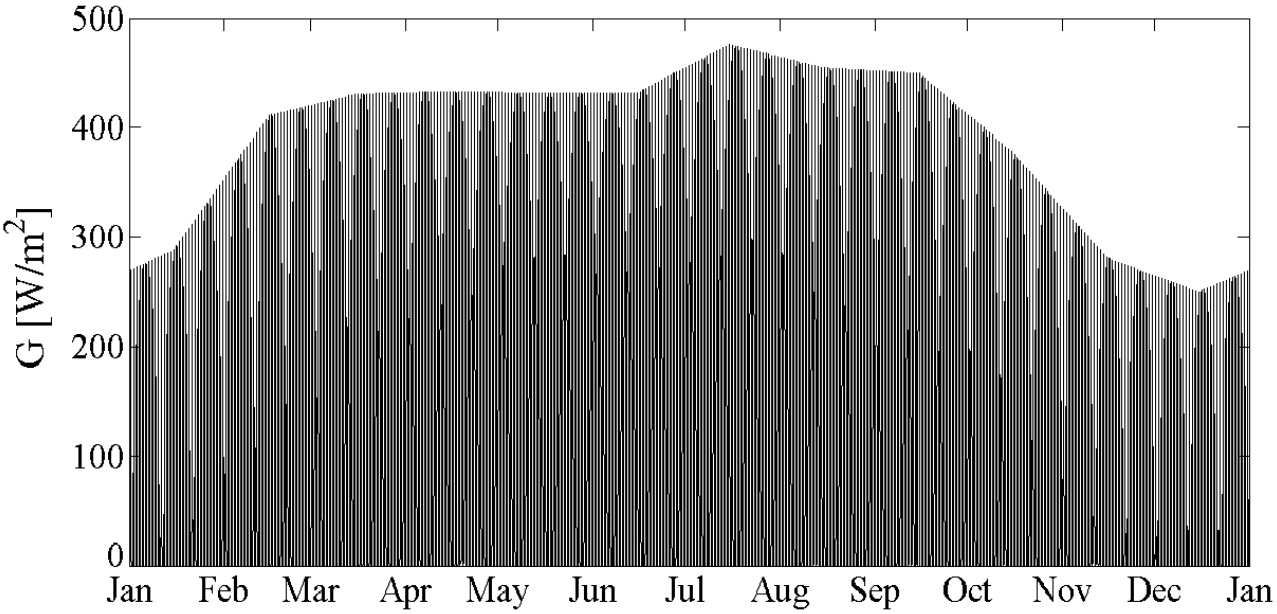
G [W/m2]
0
100
200
300
400
500
Jan
Feb
Mar
Apr
May
Jun
Jul
Aug
Sep
Oct
Nov
Dec
Jan

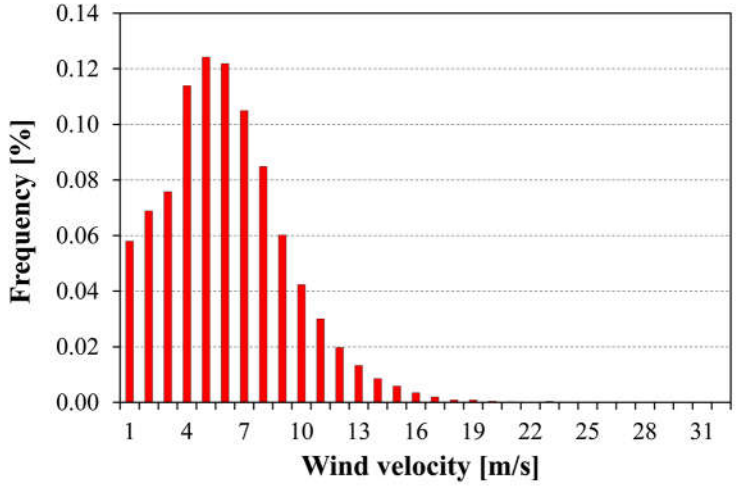
Frequency [%]
Wind velocity [m/s]
0.00
0.02
0.04
0.06
0.08
0.10
0.12
0.14
1
4
7
10
13
16
19
22
25
28
31

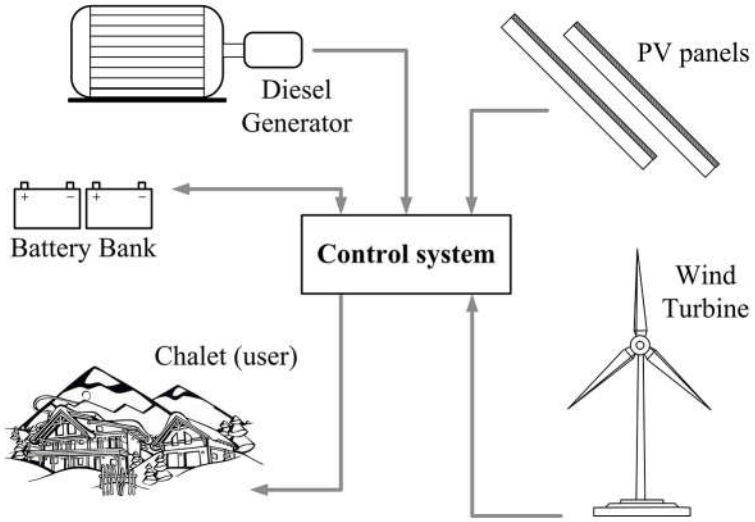
Diesel
Generator
PV panels
Battery Bank
Control system
Wind
Turbine
Chalet (user)

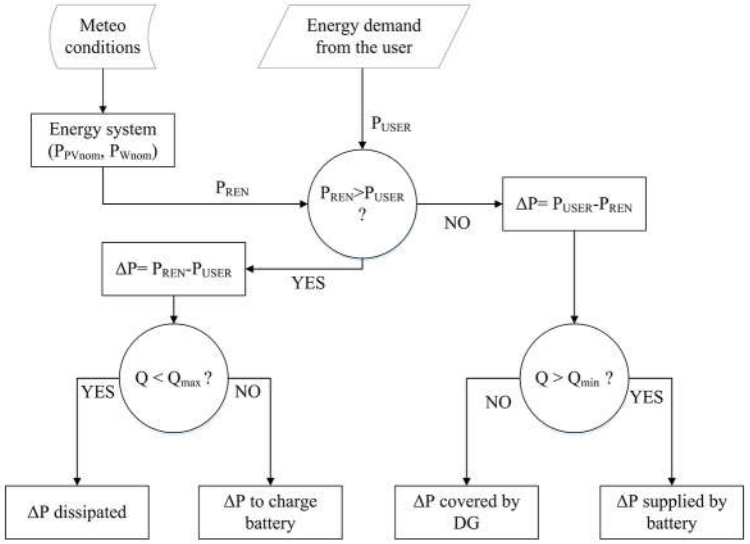
Meteo conditions
Energy demand from the user
Energy system ($P_{PVnom}$, $P_{Wnom}$)
$P_{USER}$
$P_{REN}$
$P_{REN}>P_{USER}$ ?
NO
$\Delta P= P_{USER}-P_{REN}$
YES
$\Delta P= P_{REN}-P_{USER}$
$Q < Q_{max}$ ?
YES
NO
$Q > Q_{min}$ ?
NO
YES
ΔP dissipated
ΔP to charge battery
ΔP covered by DG
ΔP supplied by battery

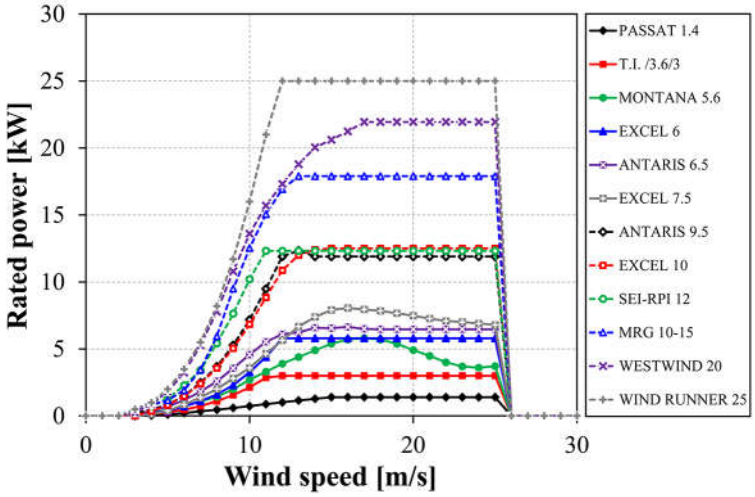
Rated power [kW]
Wind speed [m/s]
0
5
10
15
20
25
30
PASSAT 1.4
T.I. /3.6/3
MONTANA 5.6
EXCEL 6
ANTARIS 6.5
EXCEL 7.5
ANTARIS 9.5
EXCEL 10
SEI-RPI 12
MRG 10-15
WESTWIND 20
WIND RUNNER 25

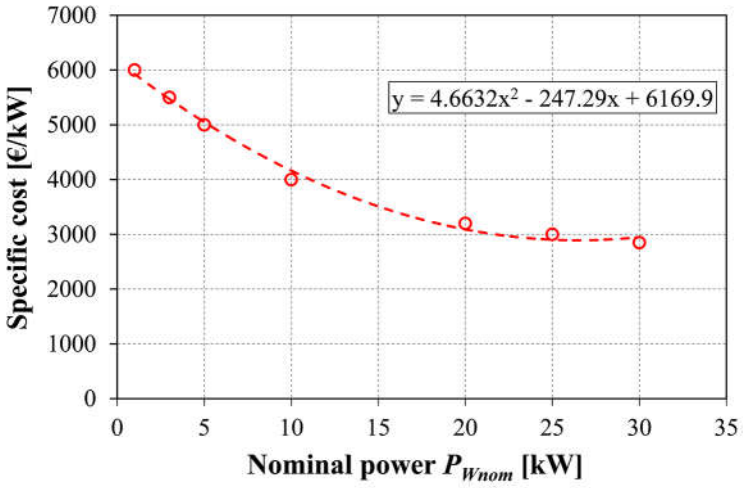
y = 4.6632x² - 247.29x + 6169.9
Specific cost [€/kW]
Nominal power $P_{Wnom}$ [kW]
7000
6000
5000
4000
3000
2000
1000
0
0
5
10
15
20
25
30
35

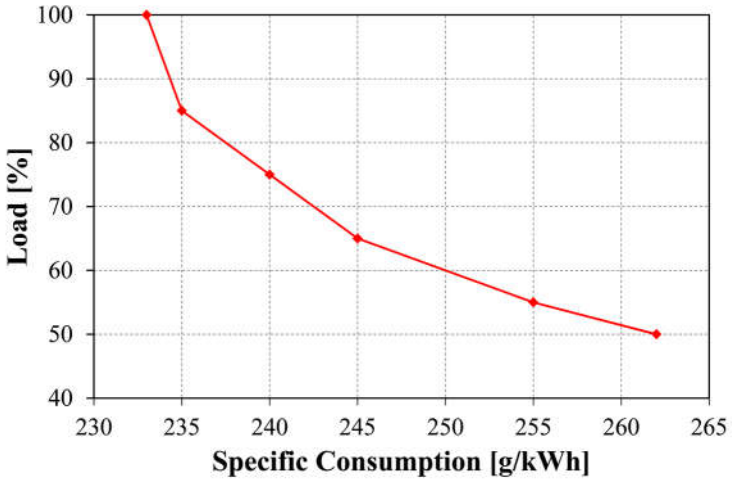
Load [%]
Specific Consumption [g/kWh]
100
90
80
70
60
50
40
230
235
240
245
250
255
260
265

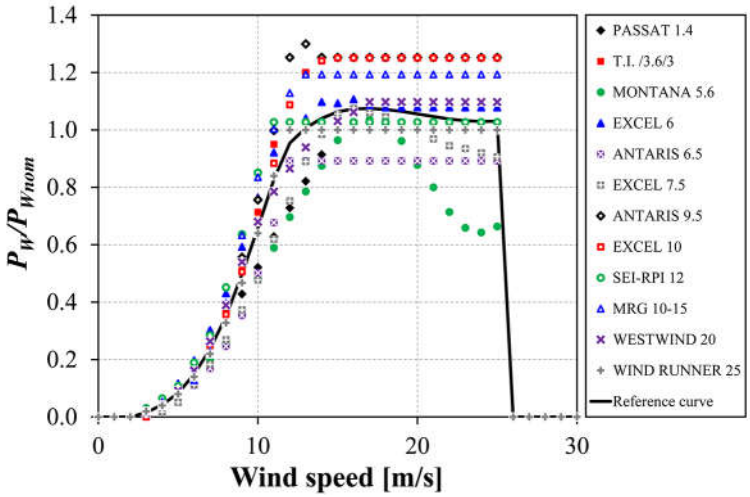
$P_W/P_{Wnom}$
Wind speed [m/s]
1.4
1.2
1.0
0.8
0.6
0.4
0.2
0.0
0
10
20
30
PASSAT 1.4
T.I. /3.6/3
MONTANA 5.6
EXCEL 6
ANTARIS 6.5
EXCEL 7.5
ANTARIS 9.5
EXCEL 10
SEI-RPI 12
MRG 10-15
WESTWIND 20
WIND RUNNER 25
Reference curve

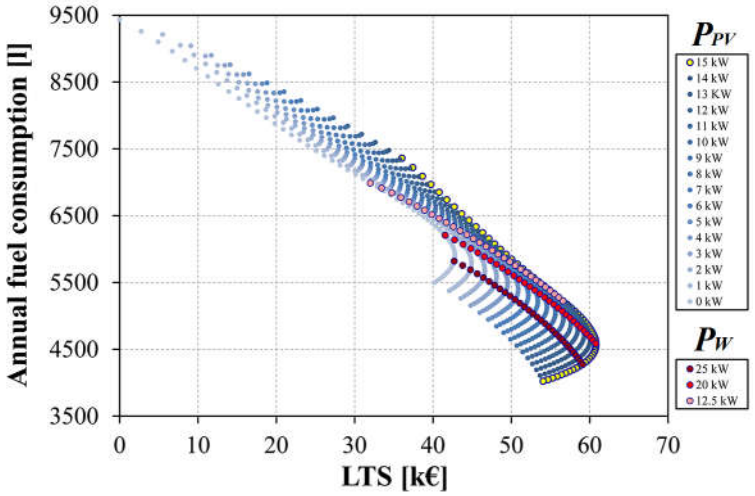
Annual fuel consumption [l]
9500
8500
7500
6500
5500
4500
3500
0
10
20
30
40
50
60
70
LTS [k€]
$P_{PV}$
15 kW
14 kW
13 KW
12 kW
11 kW
10 kW
9 kW
8 kW
7 kW
6 kW
5 kW
4 kW
3 kW
2 kW
1 kW
0 kW
$P_W$
25 kW
20 kW
12.5 kW

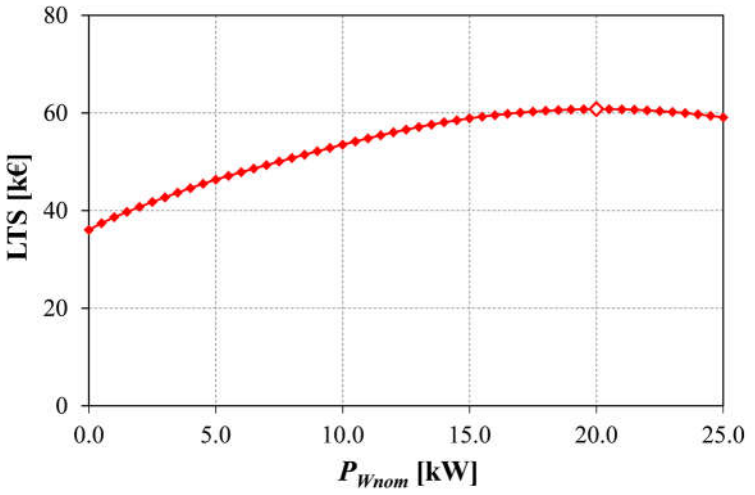
LTS [k€]
80
60
40
20
0
0.0
5.0
10.0
15.0
20.0
25.0
$P_{Wnom}$ [kW]

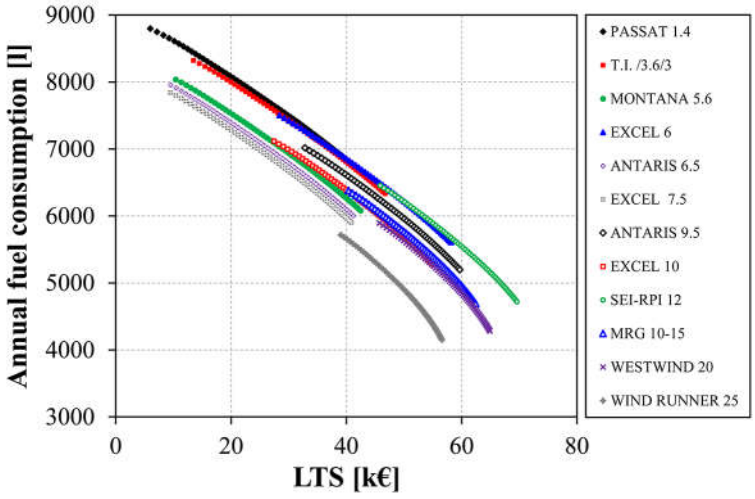
Annual fuel consumption [l]
9000
8000
7000
6000
5000
4000
3000
0
20
40
60
80
LTS [k€]
PASSAT 1.4
T.I. /3.6/3
MONTANA 5.6
EXCEL 6
ANTARIS 6.5
EXCEL 7.5
ANTARIS 9.5
EXCEL 10
SEI-RPI 12
MRG 10-15
WESTWIND 20
WIND RUNNER 25

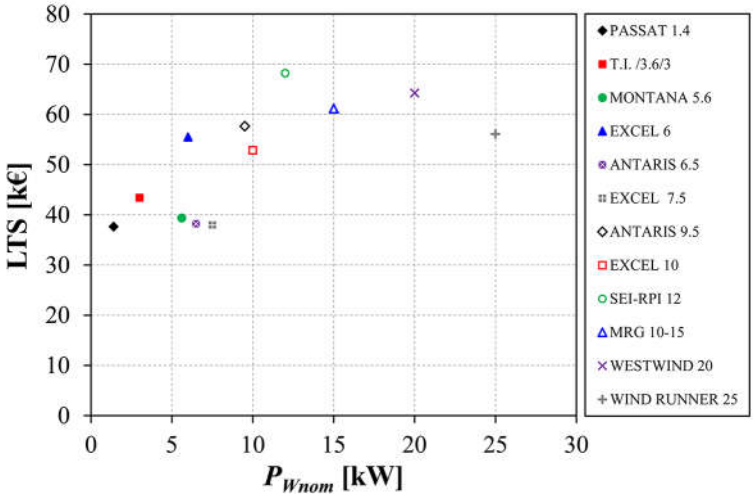
LTS [k€]
$P_{Wnom}$ [kW]
PASSAT 1.4
T.I. /3.6/3
MONTANA 5.6
EXCEL 6
ANTARIS 6.5
EXCEL 7.5
ANTARIS 9.5
EXCEL 10
SEI-RPI 12
MRG 10-15
WESTWIND 20
WIND RUNNER 25

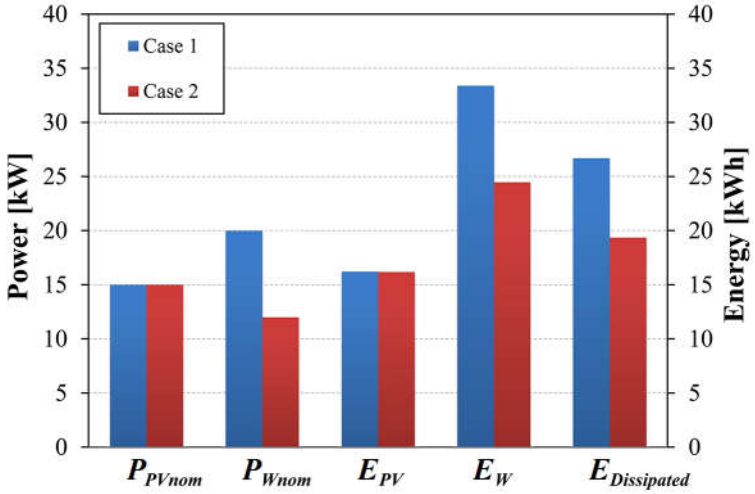
Case 1
Case 2
Power [kW]
Energy [kWh]
$P_{PVnom}$
$P_{Wnom}$
$E_{PV}$
$E_W$
$E_{Dissipated}$

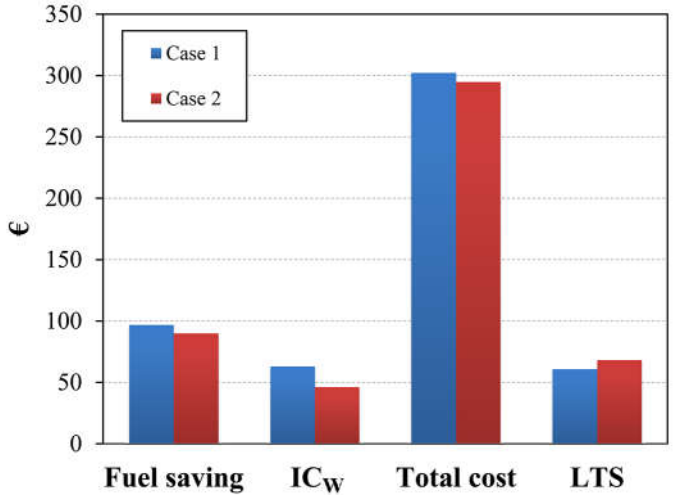
Case 1
Case 2
€
Fuel saving
$IC_W$
Total cost
LTS

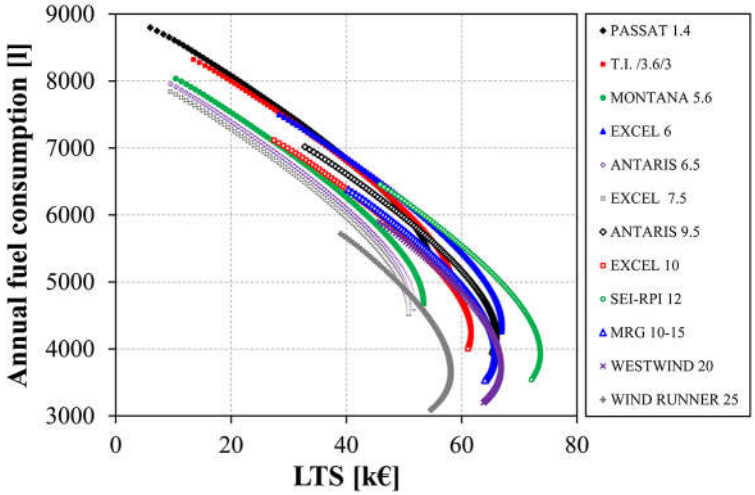
Annual fuel consumption [l]
9000
8000
7000
6000
5000
4000
3000
0
20
40
60
80
LTS [k€]
PASSAT 1.4
T.I. /3.6/3
MONTANA 5.6
EXCEL 6
ANTARIS 6.5
EXCEL 7.5
ANTARIS 9.5
EXCEL 10
SEI-RPI 12
MRG 10-15
WESTWIND 20
WIND RUNNER 25

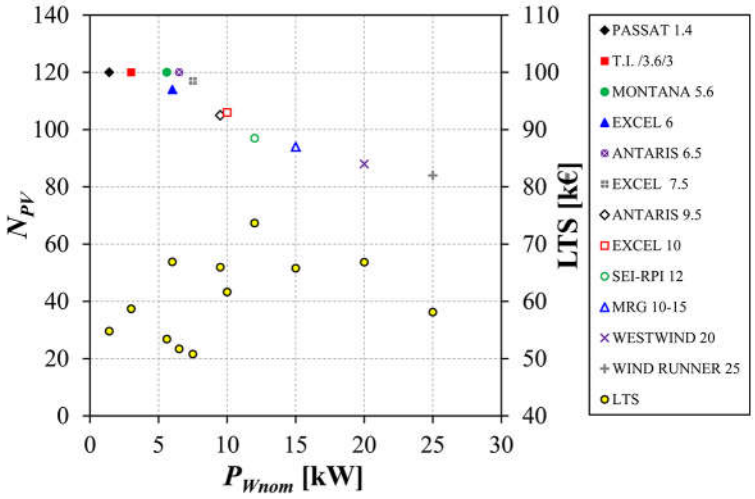
$N_{PV}$
140
120
100
80
60
40
20
0
0
5
10
15
20
25
30
$P_{Wnom}$ [kW]
LTS [k€]
110
100
90
80
70
60
50
40
PASSAT 1.4
T.I. /3.6/3
MONTANA 5.6
EXCEL 6
ANTARIS 6.5
EXCEL 7.5
ANTARIS 9.5
EXCEL 10
SEI-RPI 12
MRG 10-15
WESTWIND 20
WIND RUNNER 25
LTS

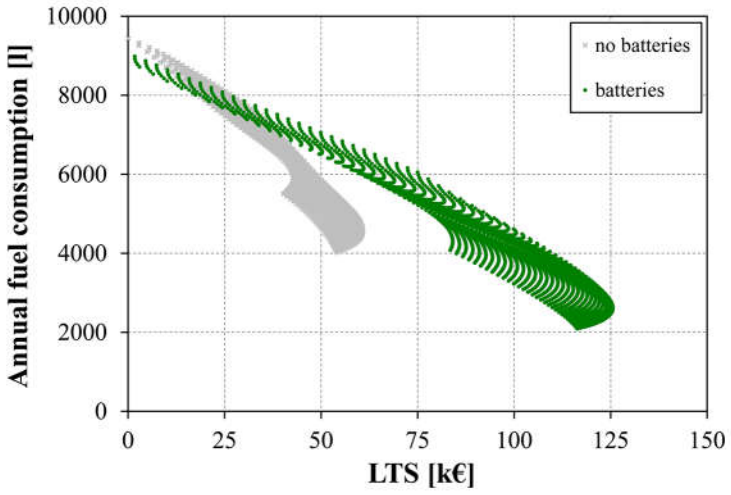
Annual fuel consumption [l]
10000
8000
6000
4000
2000
0
0
25
50
75
100
125
150
LTS [k€]
no batteries
batteries

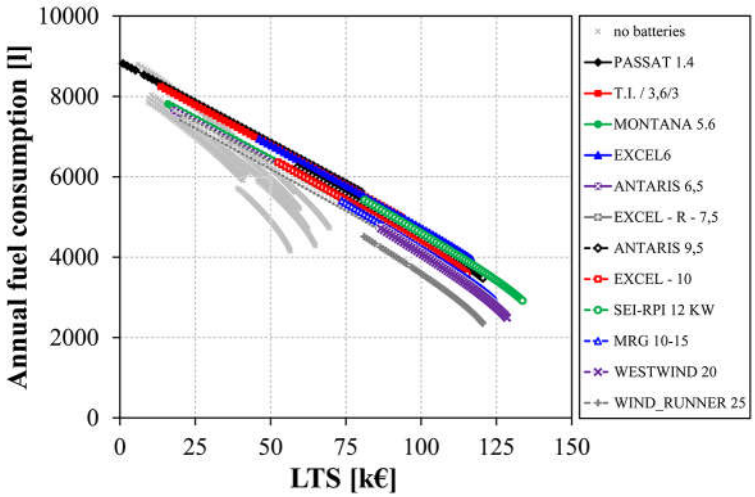
Annual fuel consumption [l]
LTS [k€]
no batteries
PASSAT 1.4
T.I. / 3,6/3
MONTANA 5.6
EXCEL6
ANTARIS 6,5
EXCEL - R - 7,5
ANTARIS 9,5
EXCEL - 10
SEI-RPI 12 KW
MRG 10-15
WESTWIND 20
WIND_RUNNER 25

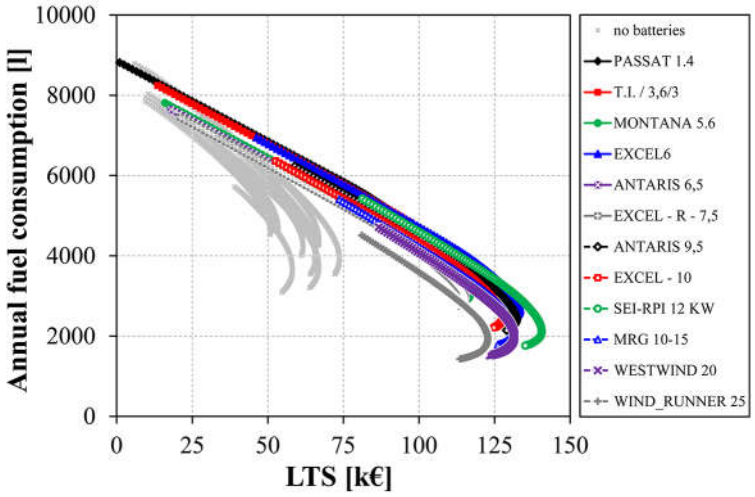
Annual fuel consumption [l]
LTS [k€]
no batteries
PASSAT 1.4
T.I. / 3,6/3
MONTANA 5.6
EXCEL6
ANTARIS 6,5
EXCEL - R - 7,5
ANTARIS 9,5
EXCEL - 10
SEI-RPI 12 KW
MRG 10-15
WESTWIND 20
WIND_RUNNER 25

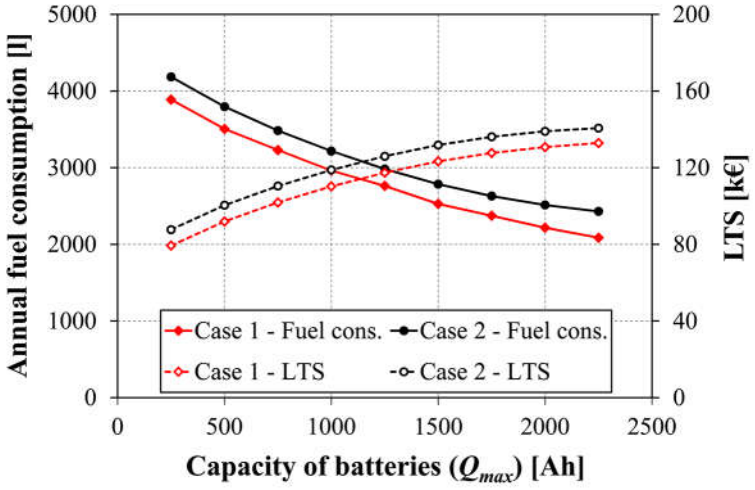
Annual fuel consumption [l]
LTS [k€]
Case 1 - Fuel cons.
Case 2 - Fuel cons.
Case 1 - LTS
Case 2 - LTS
Capacity of batteries ($Q_{max}$) [Ah]

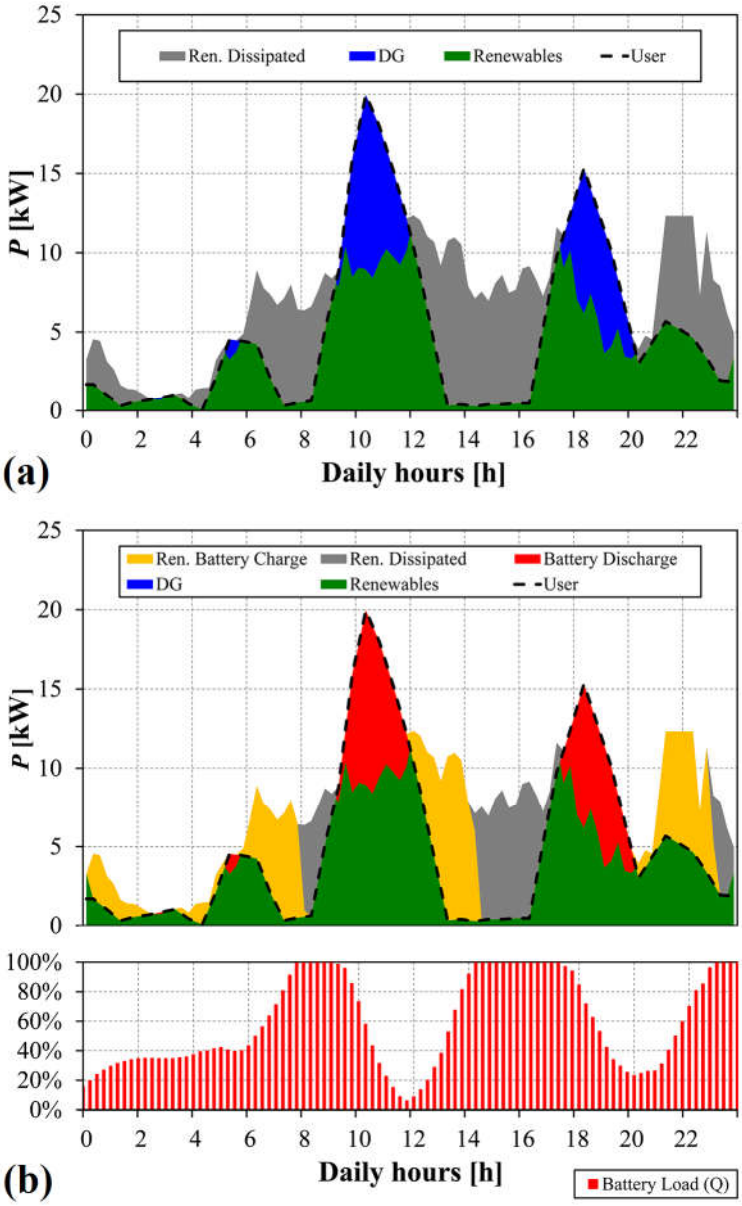
Ren. Dissipated
DG
Renewables
User
P [kW]
Daily hours [h]
(a)
Ren. Battery Charge
Ren. Dissipated
Battery Discharge
DG
Renewables
User
P [kW]
Daily hours [h]
Battery Load (Q)
(b)